Limnol. Oceanogr., 53(6), 2008, 2603–2615

A comparative study of carbon dioxide degassing in river- and marine-dominated estuaries

Li-Qing Jiang, Wei-Jun Cai,[1] *and Yongchen Wang*
Department of Marine Sciences, University of Georgia, Athens, Georgia 30602

Abstract

The partial pressure of carbon dioxide (pCO_2), concentration of total dissolved inorganic carbon, and total alkalinity were measured at both high tide and low tide in the surface water of three Georgia estuaries from September 2002 to May 2004. Of the three estuaries, Sapelo and Doboy Sounds are marine-dominated estuaries, while Altamaha Sound is a river-dominated estuary. During all sampling months, the three estuaries were supersaturated in CO_2 with respect to the atmosphere (39.5–342.5 Pa, or 390–3380 μatm) because of CO_2 inputs from within the estuarine zone (mainly intertidal marshes) and the river. Overall, pCO_2 in the river-dominated estuary is much higher than that in the marine-dominated estuaries. The calculated annual air–water CO_2 flux in Altamaha Sound (69.3 mmol m^{-2} d^{-1}) is 2.4 times those of Sapelo and Doboy Sounds (28.7–29.4 mmol m^{-2} d^{-1}). The higher CO_2 degassing in the river-dominated estuary is fueled largely by CO_2 loading from the river. Because of the substantial differences between river- and marine-dominated estuaries, current estimates of air–water CO_2 fluxes in global estuaries (which are based almost entirely on river-dominated estuaries) could be overestimated.

Recent studies have shown that estuaries are significant sources of carbon dioxide (CO_2) to the atmosphere, with partial pressure of carbon dioxide (pCO_2) varying from about 40 to 960 Pa (or ~400–9500 μatm) (Frankignoulle et al. 1998; Borges 2005; Borges et al. 2005). Even though the surface area of global estuaries is only about a 20th that of continental shelves (Woodwell et al. 1973), it is argued that CO_2 degassing by estuaries (Borges 2005; Borges et al. 2005) could nearly counterbalance the continental shelf CO_2 sink (Tsunogai et al. 1999; Borges et al. 2005; Cai et al. 2006), which is about 30–70% of the atmospheric CO_2 sink of the open ocean (1.2–1.6 Pg C yr^{-1}) (Takahashi et al. in press). However, most estuarine CO_2 studies have focused on estuaries that receive substantial freshwater discharge; much less attention has been given to estuaries that receive little freshwater discharge besides precipitation and groundwater (Frankignoulle et al. 1998; Borges 2005; Borges et al. 2005).

Definitions of estuaries vary widely. Most definitions restrict an estuary to the mouth of a river or a body of seawater reaching inland, while others argue that an estuary extends to the continental shelf (Perillo 1995). One of the most frequently cited definitions of an estuary is that of Cameron and Pritchard (1963): "a semi-enclosed coastal body of water, which has a free connection with the open sea, and within which seawater is measurably diluted with freshwater derived from land drainage." According to this definition, all river mouths and coastal brackish lagoons qualify as estuaries, although the former have been the focus for most estuarine studies.

Following Elliott and McLusky (2002), we have adopted the most widely held point of view that considers both river mouths and coastal brackish lagoons to be estuaries. The inclusion of coastal brackish lagoons as estuaries is also consistent with the fact that the most cited surface area of global estuaries was estimated "without differentiating mouths of rivers and coastal brackish lagoons" (Woodwell et al. 1973). For this study, we refer to mouths of rivers that receive significant amounts of upland river inflow as river-dominated estuaries and coastal brackish lagoons that receive little freshwater besides precipitation and groundwater as marine-dominated estuaries.

The salt marsh–surrounded estuaries of the southeastern United States cover approximately 3×10^9 m^2. River- and marine-dominated estuaries are typical features of this region, with marine-dominated estuaries covering approximately 50% of the total estuarine area in this region (National Ocean Service 1985). In this paper we present a comparative study of CO_2 in river- and marine-dominated estuaries around Sapelo Island, Georgia (Fig. 1). The proximity of these two types of estuaries and their similarities in physical conditions provide a unique opportunity to examine the CO_2 differences between these two types of estuaries. We also discuss this study's global implications on air–water CO_2 fluxes of estuaries.

Methods

Study site—Sampling was conducted in the GCE-LTER (Georgia Coastal Ecosystems—Long Term Ecological

[1] Corresponding author (wcai@uga.edu).

Acknowledgments

This work was supported by the GCE-LTER (Georgia Coastal Ecosystems—Long Term Ecological Research) program (OCE-9982133) and a NSF grant (OCE-0425153). We thank the captain and crew of R/V *Savannah* for their wonderful cooperation. Jack Blanton provided the ship time for the June 2003 cruise. We are grateful to Lawrence R. Pomeroy, Rik Wanninkhof, and Charles S. Hopkinson, who read the manuscript and gave constructive comments. The manuscript was greatly improved with the input of Jack J. Middelburg and two anonymous reviewers. We thank George Davidson and Ray Lassiter for English editing. We also thank Girong Han for laboratory support, Jack Sandow for river end-member sampling, Douglas Atkinson and Wade Sheldon for help with geographic information analysis, and Zhaohui (Aleck) Wang, Feizhou Chen, Justin Hartmann, Matt Erickson, and Ed Sheppard for help in the field.

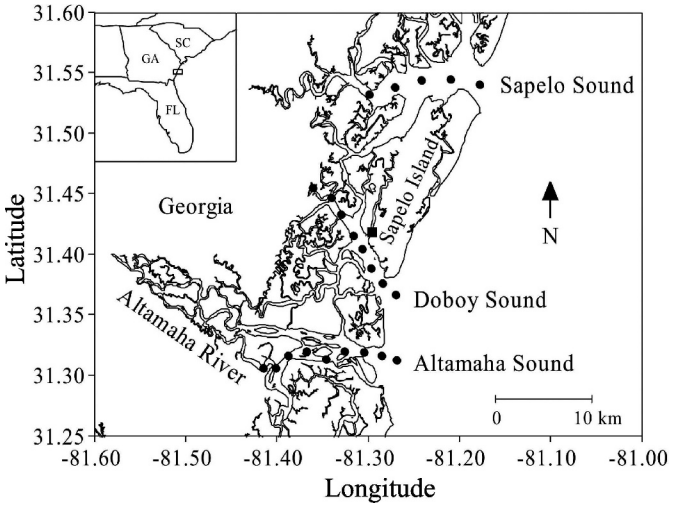

Fig. 1. Map showing the three estuaries and the sampling stations. Filled circles show the sampling stations. The sampling stations are approximately 3 km away from each other in Sapelo Sound and approximately 2 km away in Doboy and Altamaha Sounds. The filled square shows the location of Marsh Landing Climate Station.

Research) study area, which is located on the central Georgia coast of the southeastern United States (Fig. 1). This region is characterized by extensive areas of intertidal salt marshes (vegetated principally by cordgrass *Spartina alterniflora* and the rush *Juncus roemerianus*) and tidal creeks. Tides (as high as 2–3 m) flood and drain the intertidal salt marshes twice daily and transport materials back and forth into the estuaries. The Altamaha River, which is a piedmont river, is one of the largest rivers on the eastern coast of North America with a rainfall catchment area of 37,600 km^2 (Fig. 1). Discharge of the Altamaha River is usually greatest in February–April and may have a secondary peak in autumn of some years. The annual average discharge rate is 4.3–19.5 $km^3\ yr^{-1}$ (U.S. Geological Survey).

The study area in the vicinity of Sapelo Island comprises Sapelo Sound, Doboy Sound, and the Altamaha River delta (Fig. 1). The three estuaries, which have water depths of 5–15 m, experience similar physical conditions, that is, tidal amplitude, wind disturbance, solar radiation, precipitation, and so on. However, they show large differences in terms of riverine influence and salinity excursion. Sapelo Sound is a typical marine-dominated lagoonal estuary with a rainfall catchment area of approximately 150 km^2 on the lower coastal plain; Doboy Sound is also a marine-dominated coastal lagoon but receives some Altamaha River flow via the Darien River during high-flow seasons; Altamaha Sound, however, is a river-dominated estuary that receives significant amounts of freshwater from the Altamaha River (Fig. 1). Other differences among the three estuaries include Altamaha Sound having a shorter water residence time than Sapelo and Doboy Sounds because of rapid freshwater flushing and Altamaha Sound having a smaller ratio of salt marsh area to estuarine water volume than Sapelo and Doboy Sounds.

Sampling and analytical methods—Three transects in Sapelo, Doboy, and Altamaha Sounds, respectively, were surveyed during both low tide and high tide on five cruises: 16–20 September 2002, 15–21 June 2003, 01–05 December 2003, 10–16 March 2004, and 27–30 May 2004 (Fig. 1). Surface water temperature and salinity were recorded continuously with an on-board SeaBird flow-through thermosalinograph (model SBE 21) on the R/V *Savannah*. Surface water xCO_2 (mole fraction of CO_2 in the dried equilibrated carrier gas) was measured under way using a LI-COR 6252 infrared gas analyzer coupled to a gas–water equilibrator. The well-mixed gas passes through an electric Peltier cooler, which removes most of the water vapor, then a drying tube filled with magnesium perchlorate ($Mg[ClO_4]_2$) before entering LI-COR 6252. The LI-COR 6252 was calibrated every 6 h using certified gas standards, which had xCO_2 values of 200, 500, and 1000×10^{-6} referenced against standards traceable to those of the National Institute of Standards and Technology. The temperature of equilibration was measured with a Yellow Spring Instrument temperature sensor right before the equilibrator. Atmospheric xCO_2 was also measured during all cruises. Surface water and atmospheric pCO_2 were calculated by correcting the xCO_2 measurements to 100% saturation of water vapor pressure and the in situ surface water temperature (Jiang et al. 2008).

Water samples for dissolved inorganic carbon (DIC) and total alkalinity (TA) were collected at each sampling station (Fig. 1). River end-member samples were collected from JayCee Landing in Jesup, Georgia (31°67′N, 81°85′W, about 60 km upstream Altamaha Sound), on the Altamaha River. The samples were preserved with $HgCl_2$ and stored in a refrigerator on the research vessel. After the cruise, they were measured in the laboratory within 3 days. DIC concentration was determined using an automated DIC analyzer with a precision of 0.1 % (Wang and Cai 2004). A water sample of 0.5 mL was pumped into the reactor and acidified with 10% H_3PO_4. Then the extracted CO_2 gas was measured with a LI-COR 6252 infrared CO_2 detector (Wang and Cai 2004). TA was determined in a 12-mL water sample by Gran Titration to an end-point pH of 3.0. The TA titration was carried out using a computer controlled Kloehn digital pump. The precision of the TA measurement was 0.1%. Both the DIC and TA analyzers were calibrated against certified reference materials (CRMs) supplied by A.G. Dickson from Scripps Institution of Oceanography.

Temperature normalization of pCO_2—Temperature plays an important role in shaping the surface water pCO_2 by controlling the thermodynamic equilibrium of inorganic carbon system (Takahashi et al. 1993). To remove the temperature effect, pCO_2 needs to be normalized to a common temperature. Because the equation suggested by Takahashi et al. (1993) works only for open ocean water (when salinity is between 34 and 36), we used a different method to achieve temperature normalization. First, carbonate alkalinity (CA or $[HCO_3^-] + 2[CO_3^{2}]$) was calculated from pCO_2 and DIC using the inorganic carbon dissociation constants suggested for estuaries (Cai and

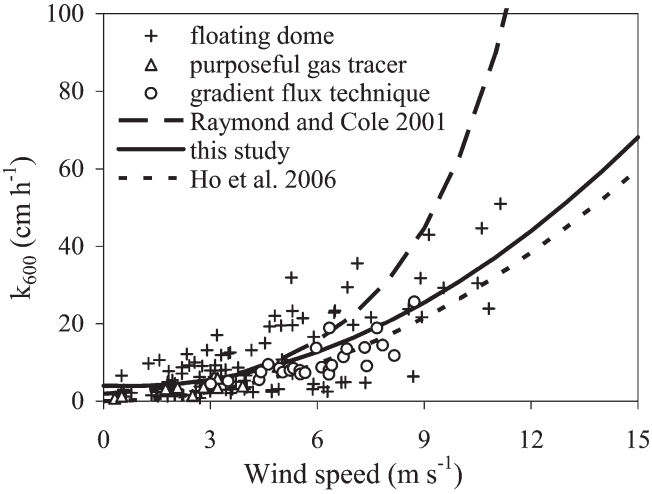

Fig. 2. k_{600} as a function of wind speed at 10 m above water surface (U_{10}). Pluses are the results from floating dome studies, open triangles are from purposeful gas tracer studies, and open circles are from gradient flux technique. The solid line is from regression of all the data. The dashed line and the dotted line are from the equations of Raymond and Cole (2001) ($k_{600} = 1.91 \times e^{0.35 \cdot U10}$) and Ho et al. (2006) ($k_{600} = 0.266 \times U_{10}^2$), respectively.

Wang 1998) at in situ temperature and salinity. Then temperature-normalized pCO_2 was calculated from the CA and DIC data using the dissociation constants at in situ salinity and the annual mean temperature of 22.63°C. The values of $(\partial pCO_2/\partial T)/pCO_2$ (T is temperature) in these estuaries were about 0.027–0.042°C^{-1}, which are less than the 0.0423°C^{-1}, as derived by Takahashi et al. (1993) for open ocean water. The values of $(\partial pCO_2/\partial T)/pCO_2$ were lowest in river-dominated estuaries at low tide and highest in marine-dominated estuaries at high tide.

Air–water CO_2 flux estimation—Air–water CO_2 flux (F, mmol m^{-2} d^{-1}) is calculated according to the following:

$$F = k \cdot K_0 \cdot (pCO_{2water} - pCO_{2air}) \quad (1)$$

where k (cm h^{-1}) is the gas transfer velocity (piston velocity) of CO_2, K_0 (mol m^{-3} Pa^{-1}) is the solubility coefficient of CO_2 at the in situ temperature and salinity, and pCO_{2water} and pCO_{2air} (Pa) are the partial pressure of CO_2 in the water and the air, respectively. A positive F indicates a transfer of CO_2 from the water to the atmosphere.

While gas transfer velocities (k) in the open ocean are dependent primarily on wind regime, those in shallow estuaries are usually more complicated. Besides the wind regime, they are also influenced by tidal current and bottom stress (Raymond and Cole 2001; Zappa et al. 2007). Consequently, the relationships of gas transfer velocity with wind speed could be site and event specific (Kremer et al. 2003; Borges et al. 2004*a*). Unfortunately, gas transfer velocities have not been widely measured in estuaries, and researchers still have to rely on wind speed dependence to approximate gas exchange rates. For this purpose, a relationship of gas transfer velocity with wind speed was produced by regressing the literature data in coastal environments (Fig. 2). The data used were mainly from the compilation by Raymond and Cole (2001), with newer measurements included (Table 1). The regressed equation is as follows:

$$k_{600} = 0.314 \cdot U_{10}^2 - 0.436 \cdot U_{10} + 3.990 \quad (2)$$

where k_{600} (cm h^{-1}) is the gas transfer velocity at the Schmidt number of 600 and U_{10} (m s^{-1}) is the wind speed referenced at 10 m above the water surface.

A comparison of Eq. 2 with that of Raymond and Cole (2001) ($k_{600} = 1.91 \times e^{0.35 \cdot U10}$) shows that when wind speeds are lower than 5 m s^{-1}, k_{600} estimated from Eq. 2 is slightly higher than that of Raymond and Cole (2001) (Fig. 2). However, when wind speeds are above 6 m s^{-1}, k_{600} from these two equations shows great differences: k_{600}

Table 1. Gas transfer velocities corrected to a Schmidt number of 600 (k_{600}) for rivers and estuaries. The measured gas transfer velocities were corrected to k_{600} using the equation provided by Wanninkhof (1992).

Study site	Method	Wind speed (m s^{-1})	k_{600} (cm h^{-1})	Reference
South San Francisco Bay	Floating dome	1.8–5.3	0.8–23.3	Hartman and Hammond (1984)
Narragansett Bay	Floating dome	1.8–3.3	4.4–11.9	Roques (1985)
Hudson River	Floating dome	0.6–6.5	2.9–23.4	Marino and Howarth (1993)
Hudson River	Purposeful gas tracer	2.5–4.9	1.5–9.0	Clark et al. (1994)
Parker River	Purposeful gas tracer	0.3–2.1	0.8–3.5	Carini et al. (1996)
Two estuaries near Waquoit Bay, Massachusetts	Floating dome	0.4–8.7	1.2–6.4	Kremer et al. (2003)
Randers Fjord, Scheldt and Thames Estuaries (Europe)	Floating dome	0.5–11.1	2.1–51.0	Borges et al. (2004*a*)
Scheldt Estuary (Europe)	Floating dome	1.8–10.5	7.7–30.5	Borges et al. (2004*b*)
Sinnamary River and Estuary (French Guiana)	Floating dome	0.5–4.7	6.6–19.3	Guérin et al. (2007)*
Fukido River, Japan	Floating dome	2.0–4.0	1.7–8.7	Tokoro et al. (2007)
Parker and Hudson River	Gradient flux technique	3.0–8.7	4.4–25.7	Zappa et al. (2007)

*Averaged over wind speed bins of 1 m s^{-1}.

calculated from Eq. 2 tends to follow the trend in the open ocean (Wanninkhof 1992; Ho et al. 2006), while that from the exponential relationship of Raymond and Cole (2001) becomes considerably higher (Fig. 2).

The equation of Raymond and Cole (2001) was obtained by an exponential regressing of available literature data in rivers and estuaries from that time. Most of the data used were measured when wind speeds were lower than 7 m s^{-1}. While the equation reasonably estimates gas transfer velocities when wind speeds are low, it could substantially overestimate gas transfer velocities when extrapolated to high wind speeds (Fig. 2). Since wind speeds during this study are up to 12 m s^{-1}, we used Eq. 2 instead of that of Raymond and Cole (2001) to estimate air–water CO_2 fluxes.

Wind speeds obtained at 10 m height from the Marsh Landing Climate Station located on Sapelo Island, Georgia (Fig. 1) were used to calculate k_{600} from Eq. 2. While the Marsh Landing Climate Station is very close to Doboy Sound, it is about 12–15 km from the sampling stations in Sapelo and Altamaha Sounds (Fig. 1). After k_{600} was estimated from wind speeds, the gas transfer velocities at in situ temperature were calculated as follows:

$$k_{\mathrm{SST}} = k_{600} \times \left(\frac{Sc_{\mathrm{SST}}}{600}\right)^{-0.5} \quad (3)$$

where k_{SST} is the gas transfer velocity at the sea surface temperature and Sc_{SST} is the Schmidt number of CO_2 at the sea surface temperature (Wanninkhof 1992).

To estimate area-averaged CO_2 fluxes, the surveyed areas of the estuaries were divided into five to eight segments, with each segment centered by one of the sampling stations (Fig. 1). The area-averaged flux in each estuary was then calculated as follows:

$$F_{\mathrm{area-averaged}} = \frac{\sum F_i \cdot S_i}{\sum S_i} \quad (4)$$

where $F_{\mathrm{area\text{-}averaged}}$ is the area-averaged flux in the estuary, F_i is the average of all the fluxes within segment i, and S_i is the surface area of segment i. The fluxes in months when pCO_2 was not measured were approximated by assuming a linear seasonal change of pCO_2. Since wind speeds were fairly constant in all months, this is equivalent to a linear seasonal change of gas fluxes. The annual fluxes were calculated as the average of all the monthly fluxes. Here one needs to keep in mind that the assumption of a linear seasonal change is not necessarily the case in the field and thus could cause uncertainties.

Results

Hydrographic data—Surface water temperature did not show noticeable differences between high tide and low tide and was very similar among the three estuaries in all sampling months. It was 14–15°C during the March 2004 and December 2003 cruises and 27–29°C during the May 2004, June 2003, and September 2002 cruises (Fig. 3a).

The Altamaha River discharged the most water during March 2004 and June 2003 (high-flow months) and the least during May 2004, September 2002, and December 2003 (low-flow months) (Fig. 3b). Of the two high-flow months, June 2003 showed discharge rates that were significantly higher than the long-term average (Fig. 3b).

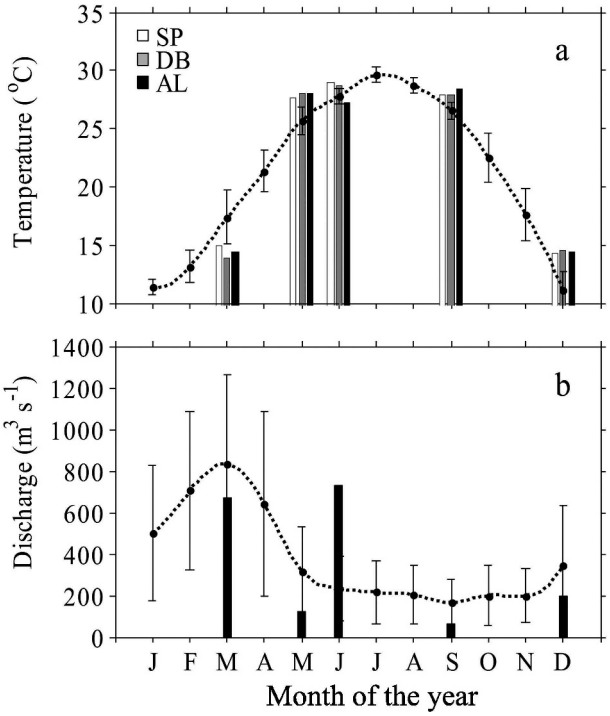

Fig. 3. Surface water temperature and Altamaha River discharge rates. Columns in (a) show surface water temperature in the three estuaries during the sampling months of March 2004, May 2004, June 2003, September 2002, and December 2003. Open columns are for Sapelo Sound (SP), gray columns are for Doboy Sound (DB), and black columns are for Altamaha Sound (AL). Filled circles and dotted line in (a) are the average water temperature from 2002 to 2005. Columns in (b) show Altamaha River discharge rates during all sampling months. Filled circles and dotted line in (b) are the 30-yr average discharge rates from 1976 to 2005.

The surface water salinity measurements confirm the various freshwater influences on the three estuaries (Fig. 4). Sapelo and Doboy Sounds were rarely influenced by freshwater runoff, although Doboy Sound received slight freshwater input during the high-flow months of March 2004 and June 2003 (Fig. 4). On the contrary, Altamaha Sound showed surface water salinity that is typical of river-dominated estuaries (Fig. 4).

Surface water pCO_2—During all sampling months, the three estuaries were supersaturated in CO_2 with respect to the atmosphere (atmospheric xCO_2: 371–389 $\times$ 10^{-6}), with surface water pCO_2 ranging from 39.5 to 342.5 Pa (Fig. 5). Some shared characteristics of the pCO_2 in the three estuaries include surface water pCO_2 being lowest at the ocean end and increased toward the innermost area of the estuaries and surface water pCO_2 at low tide always being higher than at high tide for any given point in space, although the difference is barely noticeable for a given salinity value.

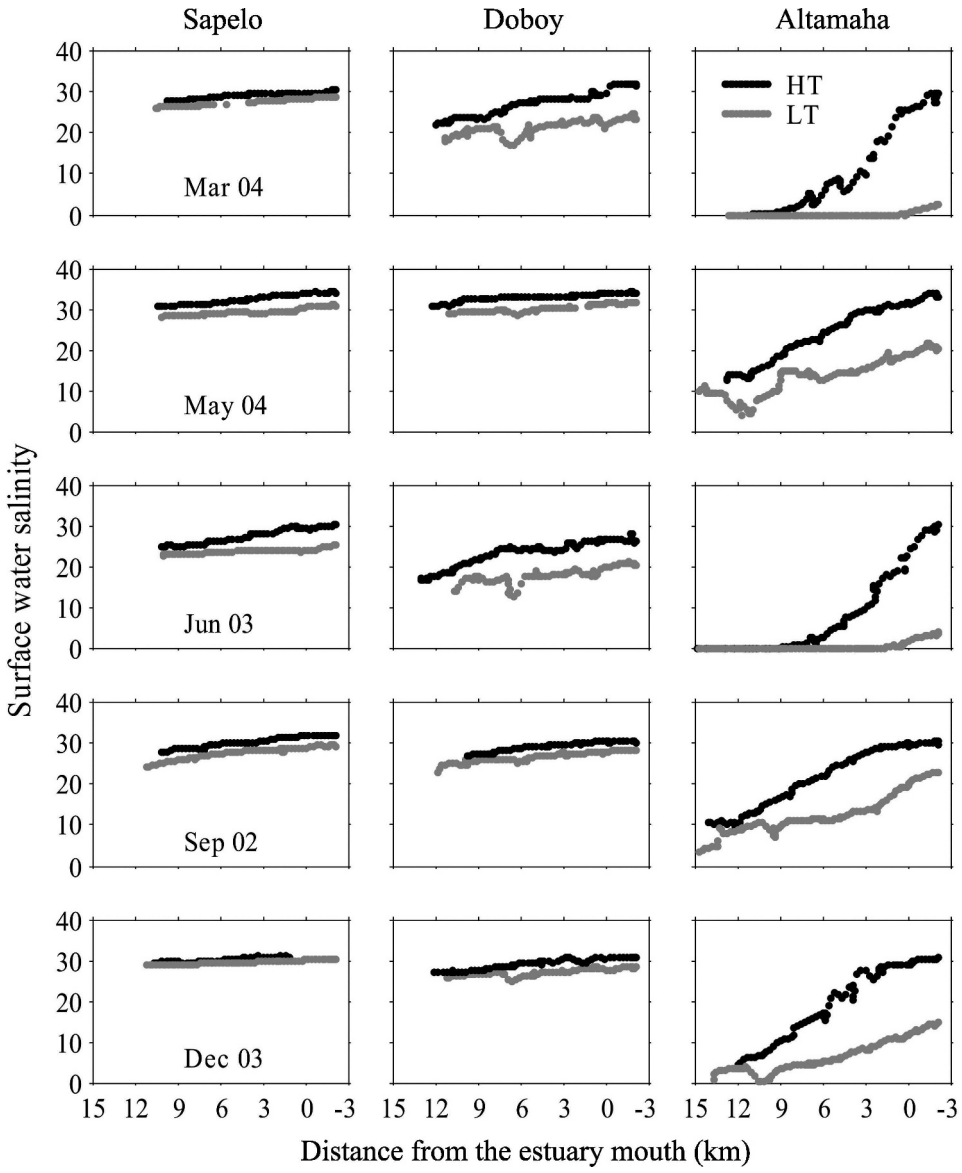

Fig. 4. Spatial distributions of surface water salinity in the three estuaries during both high tide and low tide in all the sampling months. Black dots are the salinity at high tide (HT), and gray dots are the salinity at low tide (LT). For the x-axis, positive values are inland, and negative values are out to sea.

Surface water pCO_2 in the two marine-dominated estuaries (Sapelo and Doboy Sounds) showed similar seasonal variations as that in the Duplin River, a nearby blind tidal creek that receives no freshwater besides precipitation and groundwater (Wang and Cai 2004). pCO_2 in Sapelo and Doboy Sounds was lowest in the cold months of March 2004 and December 2003 and highest in the warm months of June 2003 and September 2002 (Fig. 5). Spatially, pCO_2 showed the largest magnitude of seasonal change in the innermost area of Sapelo and Doboy Sounds (Fig. 5).

Surface water pCO_2 in the river-dominated estuary of Altamaha Sound was always higher than that in the two marine-dominated estuaries during all sampling months (Fig. 5). The highest pCO_2 in Altamaha Sound was 342.5 Pa compared to 243.2 Pa in Sapelo and Doboy Sounds. Surface water pCO_2 in Altamaha Sound contrasted seasonally with that in the two marine-dominated estuaries. pCO_2 in Altamaha Sound peaked during the high-flow months of March 2004 and June 2003, although in the low-flow months, it showed seasonal variations similar to those in the two marine-dominated estuaries (Fig. 5).

Air–water CO_2 fluxes—The calculated air–water CO_2 fluxes in the three estuaries were always positive (releasing CO_2 to the air) during all sampling months (Table 2). Fluxes at low tide were always higher than those at high tide. Fluxes averaged over high and low tide in the three estuaries ranged from 9 to 128 mmol m^{-2} d^{-1}. The annual

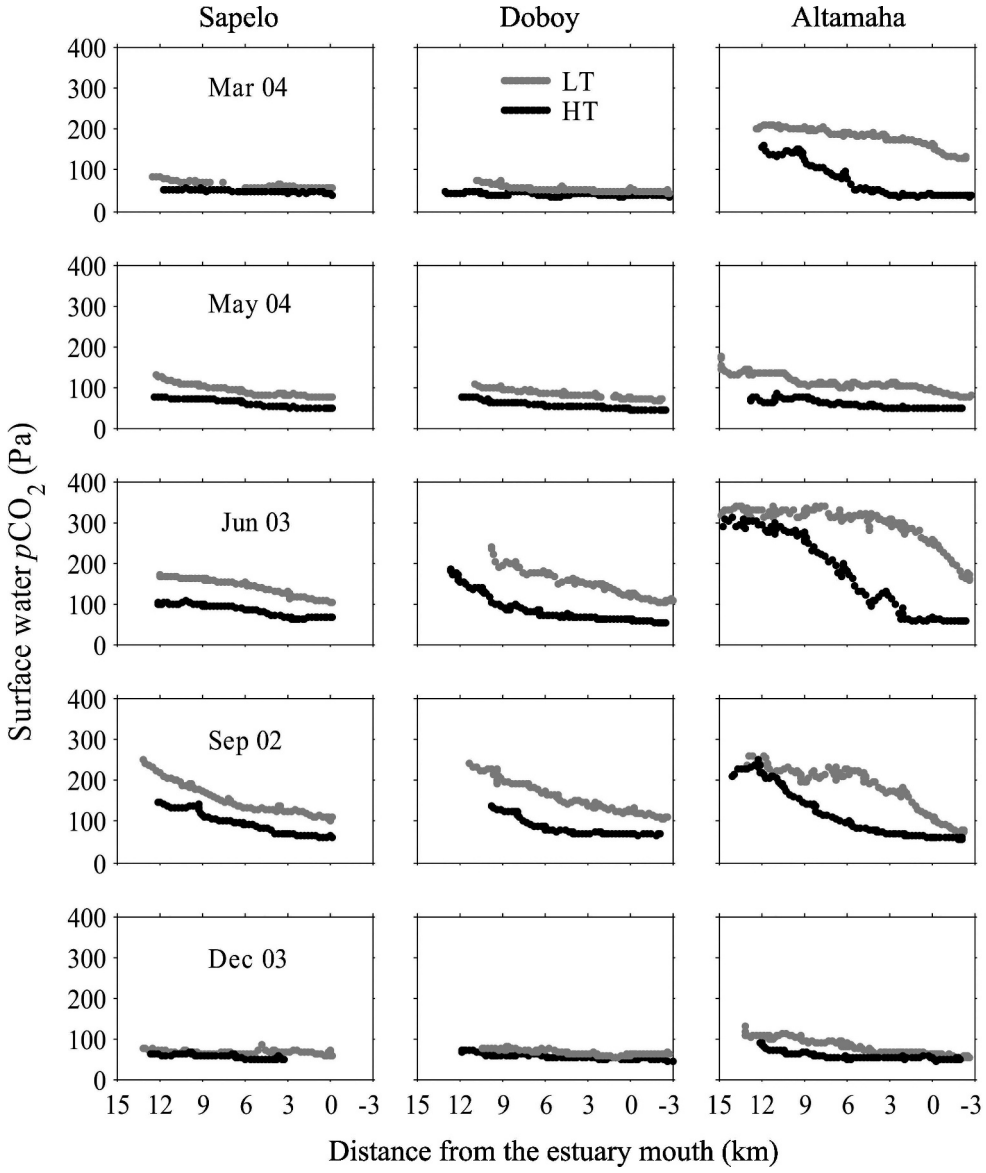

Fig. 5. Surface water pCO_2 in the three estuaries during both high tide and low tide in all the sampling months. Gray dots are the pCO_2 at low tide (LT), and black dots are the pCO_2 at high tide (HT). For the x-axis, positive values are inland, and negative values are out to sea.

average air–water CO_2 flux of Altamaha Sound was 69.3 mmol m^{-2} d^{-1}, which is about 2.4 times that of the two marine-dominated estuaries (Sapelo and Doboy Sounds), where the fluxes were 28.7 and 29.4 mmol m^{-2} d^{-1}, respectively (Table 2).

One of the biggest uncertainties in the air–water CO_2 fluxes comes from the uncertainty in estimating gas transfer velocity. The monthly averaged gas transfer velocities based on field wind speeds during this study varied from 7.7 to 8.6 cm h^{-1} (Table 2). They are at the higher end of 3.0–7.0 cm h^{-1} as suggested for estuaries by Raymond and Cole (2001) and at the lower end of the 8.7–17.1 cm h^{-1} as estimated by Elsinger and Moore (1983) using the ^{222}Rn and ^{226}Ra disequilibria method in a nearby river—Pee Dee River, South Carolina. The generic relationship of gas transfer velocity as a function of wind speed in estuaries introduces large errors in gas transfer velocity (Borges et al. 2004*a*). Consequently, air–water CO_2 fluxes of this study might suffer from large uncertainties.

This uncertainty, however, should not affect the conclusion that CO_2 degassing in Altamaha Sound was much higher than that in Sapelo and Doboy Sounds. During the flux calculation, the same gas transfer velocity (k_{600}) was used for all three estuaries in the same sampling month (Table 2). In terms of key factors controlling gas transfer velocity in an estuary (wind speeds, tidal amplitude, bottom stress, and fetch; Borges et al. 2004*a*; Zappa et al. 2007), these three estuaries are similar. Gas transfer velocities in Altamaha Sound could be slightly higher than those in the two marine-dominated estuaries because of added turbulence caused by discharge enhanced velocities in Altamaha Sound. This factor would strengthen the

Table 2. Area-averaged air–water CO_2 fluxes (mmol m^{-2} d^{-1}) in Sapelo, Doboy, and Altamaha Sounds during all the sampling months. "HT," "LT," and "Avg." are high tide, low tide, and the average of high tide and low tide, respectively. The bottom row of the table shows the gas transfer velocities (k_{600}) used to calculate the fluxes.

Estuaries	Tide	Mar 2004	May 2004	Jun 2003	Sep 2002	Dec 2003	Annual average
Sapelo Sound	HT	8.3	15.1	24.6	31.0	12.9	18.7
	LT	19.3	33.6	57.3	63.1	20.8	38.7
	Avg.	13.8	24.3	41.0	47.0	16.8	28.7
Doboy Sound	HT	4.2	12.2	23.9	29.1	12.8	16.8
	LT	14.0	30.4	71.2	72.7	21.0	42.0
	Avg.	9.1	21.3	47.5	50.9	16.9	29.4
Altamaha Sound	HT	43.5	16.8	86.8	51.7	19.2	43.4
	LT	112.4	58.2	169.0	107.9	37.5	95.2
	Avg.	78.0	37.5	127.9	79.8	28.4	69.3
k_{600} (cm h^{-1})	—	8.6	8.3	7.7	7.7	8.5	8.1

conclusion that Altamaha Sound has higher air–water CO_2 fluxes.

DIC—DIC concentrations in the two marine-dominated estuaries (Sapelo and Doboy Sounds) ranged from 1500 to 2200 μmol kg^{-1} (Fig. 6). Spatial patterns of DIC concentration in Sapelo and Doboy Sounds varied seasonally. DIC concentration was higher in the innermost area of the sounds than at the ocean end during the low-flow months of May 2004, September 2002, and December 2003 (Fig. 6). This trend was reversed during the high-flow months of March 2004 and June 2003. The seasonal changes in spatial DIC distributions in the two marine-dominated estuaries are easier to observe in Doboy Sound, which receives more freshwater than Sapelo Sound during high-flow months (Fig. 6).

DIC concentrations in Altamaha Sound showed much larger spatial and seasonal variations (450–2100 μmol kg^{-1}) compared to the two marine-dominated estuaries (Fig. 6). The DIC concentration always increased toward the ocean end. It increased almost linearly with salinity because of fast flushing of the estuary, although the external inputs of DIC during mixing can be seen from the upward curvature of the DIC vs. salinity plots (Fig. 6). The nonconservative DIC inputs, however, are less noticeable than those observed in the Satilla River Estuary, which has a longer water residence time (Cai and Wang 1998). Seasonally, DIC concentrations in Altamaha Sound were controlled mainly by river discharge rates. They were lowest when river discharge rates were at their highest. Overall, DIC concentrations farthest upstream of Altamaha Sound showed the largest seasonal variations. Finally, a comparison of DIC at the river end member (JayCee Landing in Jesup, Georgia) with the DIC at zero salinity within the estuary suggests that DIC sources in the 60-km freshwater stretch are also significant during low-flow months (Fig. 6).

Discussion

Estuarine pCO_2 is controlled by seasonal changes of water temperature and net CO_2 inputs from (1) the ocean, (2) the river, and (3) within the estuarine zone. Temperature is important in the thermodynamic equilibrium of inorganic carbon system: it increases pCO_2 in summer and fall and decreases pCO_2 in winter and spring in the northern hemisphere. CO_2 addition processes in the estuarine zone include net ecosystem metabolism within the estuary, DIC transport between surrounding intertidal marshes and the estuary, groundwater input, air–water gas exchange, calcium carbonate formation or dissolution, and all other processes within the estuarine zone that could contribute to the gain or loss of CO_2 except those of the river and the ocean. In the following sections, the different CO_2 controlling mechanisms in the three estuaries of the southeastern United States coast (marine vs. river dominated) are discussed.

CO_2 in marine-dominated estuaries—pCO_2 in the two marine-dominated estuaries (Sapelo and Doboy Sounds) was lowest in winter and spring and highest in summer and fall. The seasonal changes of pCO_2 in these estuaries are controlled mainly by the annual cycle of water temperature and the seasonal net CO_2 inputs from within the estuarine zone.

After temperature normalization, pCO_2 of the two marine-dominated estuaries is still higher in the warm months of June and September than in other months (Fig. 7). Comparisons of in situ pCO_2 with the corresponding temperature-normalized pCO_2 show that water temperature lowers or raises the pCO_2 value by 20–30% in winter and summer, respectively, during the sampling months.

We estimated the net DIC input from within the estuarine zone by modifying the approach of Cai et al. (2003). At any sampling station, the DIC in excess of that from mixing of the river and ocean end members (DIC_{excess}) can be expressed as follows:

$$DIC_{excess} = DIC_i - DIC_{mixing} \quad (5)$$

where DIC_i is the DIC concentration of station i and DIC_{mixing} is the DIC concentration due to mixing of the ocean and freshwater end members.

DIC_{mixing} can be estimated from the DIC mixing line using the end-member data (Fig. 8a). When inputs of DIC from the river are negligible, for example, during all

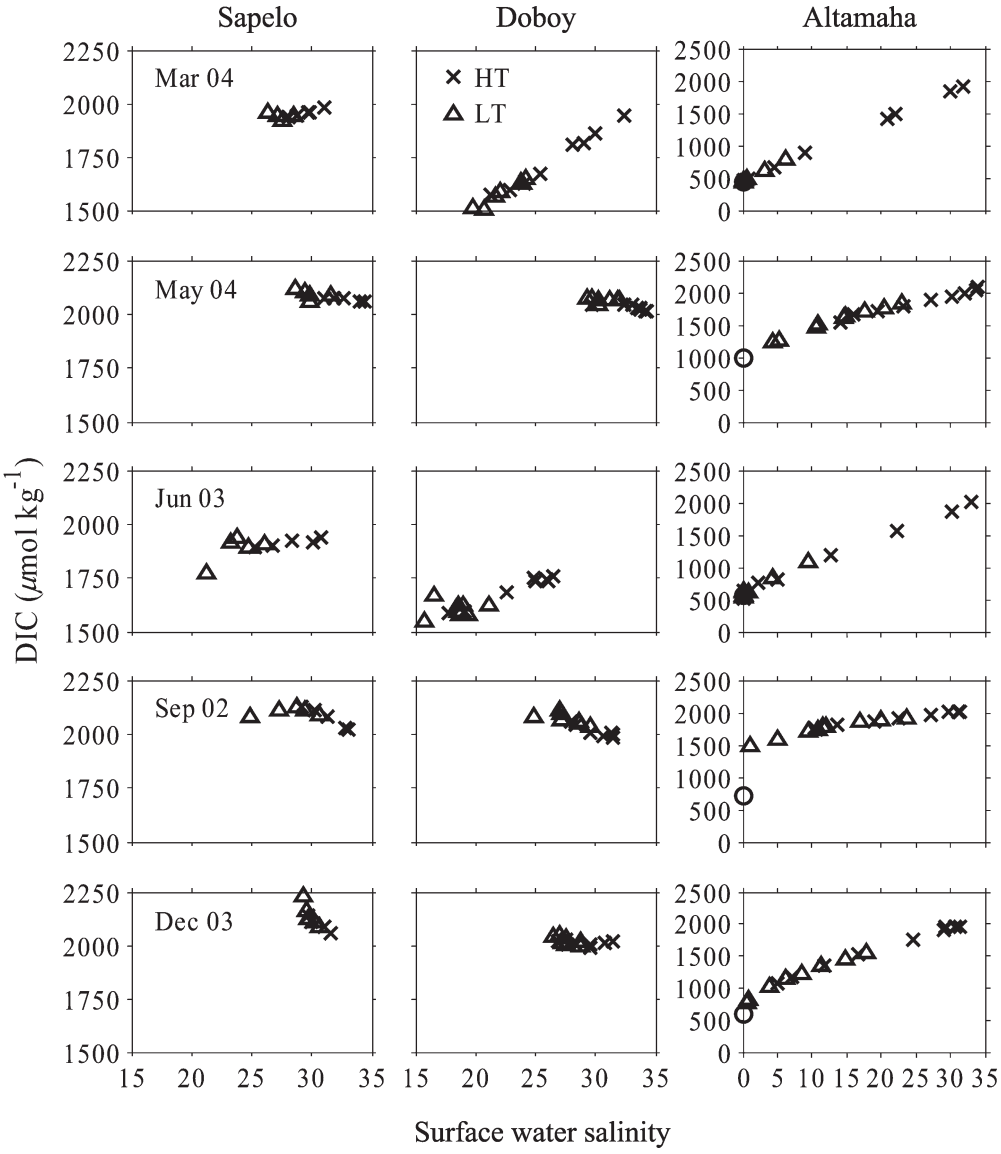

Fig. 6. Dissolved inorganic carbon (DIC) vs. surface water salinity in the three estuaries during both high tide and low tide in all the sampling months. Crosses are DIC at high tide (HT), and triangles are DIC at low tide (LT). Circles in the rightmost panels are DIC of the river end member from JayCee Landing in Jesup, Georgia. During high-flow months (e.g., March 2004 and June 2003), the end-member data may not be visible because they are close to the value within the estuary at zero salinity.

sampling months in Sapelo Sound and low-flow months in Doboy Sound, DIC_{mixing} can be calculated as follows (Fig. 8a):

$$DIC_{mixing\,w/o} = \frac{S_i}{S_{ocean}} \cdot DIC_{ocean} \quad (6)$$

where $DIC_{mixing\ w/o}$ is the DIC concentration after the ocean end member is diluted only by a zero DIC freshwater and S_i and S_{ocean} are the salinity of station i and the ocean end member, respectively. When Eq. 6 is used to calculate DIC_{mixing}, the estimated DIC_{excess} also includes any possible DIC input from the river.

When inputs of DIC from the river are significant, for example, during all months in Altamaha Sound and the high-flow months in Doboy Sound, DIC_{mixing} has a substantial contribution from freshwater and can be calculated as follows (Fig. 8a):

$$DIC_{mixing\,w/R} = \frac{S_i}{S_{ocean}} \cdot DIC_{ocean} + \left(1 - \frac{S_i}{S_{ocean}}\right) \cdot DIC_{river} \quad (7)$$

where $DIC_{mixing\ w/R}$ is the DIC concentration after mixing of the ocean and the river end members, and DIC_{river} is the DIC concentration of the river end member.

The excess DIC results show that during all sampling months in Sapelo Sound and the low-flow months in

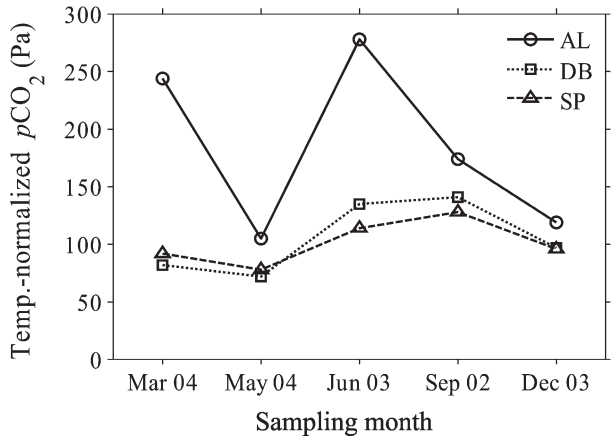

Fig. 7. Temperature-normalized surface water pCO_2 (T = 22.63°C) in the three estuaries (area averaged) at low tide in all the sampling months. Circles and solid line are temperature-normalized pCO_2 in Altamaha Sound (AL), squares and dotted line are temperature-normalized pCO_2 in Doboy Sound (DB), and triangles and dashed line are temperature-normalized pCO_2 in Sapelo Sound (SP).

Doboy Sound, excess DIC is lowest in winter and spring and highest in summer and fall. Plots of temperature-normalized pCO_2 against excess DIC show that excess DIC is responsible for the spatial and seasonal variations of the temperature-normalized pCO_2 in the two marine-dominated estuaries (Fig. 9). During the high-flow months of March 2004 and June 2003 in Doboy Sound, excess DIC is lower than that of Sapelo Sound because of the shorter residence time of Doboy Sound caused by river flushing (Fig. 9). Regulations of CO_2 in Doboy Sound during these high-discharge months are more like those in river-dominated estuaries, which will be discussed later. Temperature-normalized pCO_2 in the river-dominated estuary (Altamaha Sound) is not correlated with excess DIC except for September 2002, when Altamaha Sound behaves similarly to a marine-dominated estuary because of the low river discharge and high water temperature (Fig. 9).

Excess DIC in these estuaries is the sum of all DIC inputs from within the estuarine zone. Earlier studies argued that in these salt marsh–surrounded estuaries, direct CO_2 input from the surrounding intertidal marshes is one of the most important excess DIC sources (Cai et al. 1999; Neubauer and Anderson 2003; Wang and Cai 2004).

The southeastern coast of the United States has large areas of intertidal salt marshes dominated by *S. alterniflora*, which has a high productivity of about 1100–2200 g C m^{-2} yr^{-1} (Dai and Wiegert 1996). After the *Spartina* dies, a large fraction of the organic matter decomposes in situ. Dissolved organic carbon exuded from the marsh grasses during growth also contributes to the decomposition. Some of the CO_2 produced in the intertidal marsh water and sediment (Middelburg et al. 1996) will be mixed into estuarine water via tidal oscillation (Neubauer and Anderson 2003) and drainage of marsh sediment interstitial water (Jahnke et al. 2003). This is the major mechanism fueling the high CO_2 degassing in these estuaries (Cai and Wang 1998; Cai et al. 1999; Wang and Cai 2004).

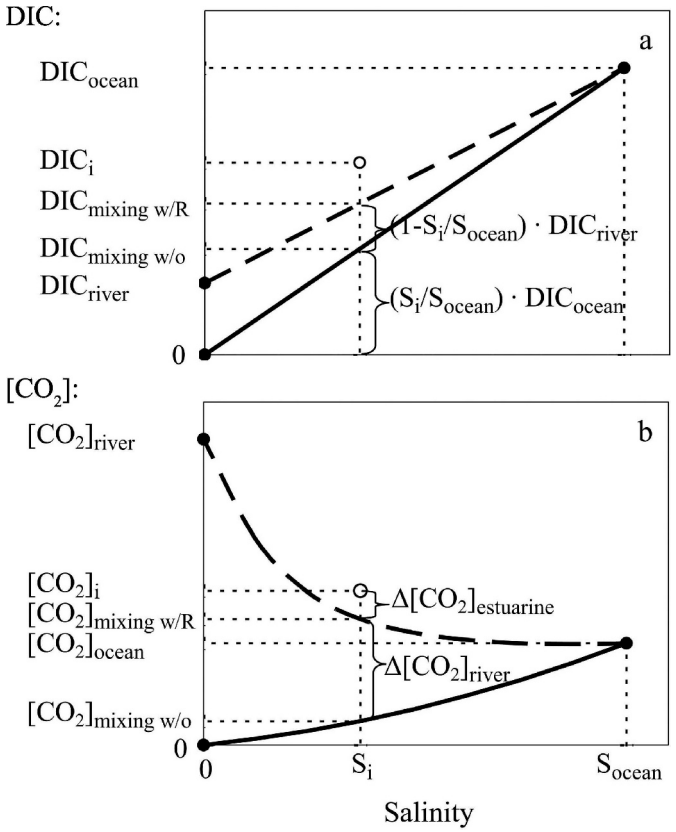

Fig. 8. Diagrams showing DIC and dissolved CO_2 concentrations during estuarine mixing. (a) DIC concentrations during estuarine mixing. On the x-axis, S_i and S_{ocean} are salinity of station i and the ocean end member, respectively. On the y-axis, DIC_{ocean}, DIC_i, and DIC_{river} are DIC of the ocean end member, station i, and the river end member, respectively. $DIC_{mixing\ w/R}$ is DIC after conservative mixing of the ocean and river end members, and $DIC_{mixing\ w/o}$ is DIC after the ocean end member is diluted only by a zero DIC freshwater. (b) Dissolved CO_2 concentrations during estuarine mixing. On the y-axis, $[CO_2]_{river}$, $[CO_2]_i$, and $[CO_2]_{ocean}$ are dissolved CO_2 concentration of the river end member, station i, and the ocean end member, respectively. $[CO_2]_{mixing\ w/R}$ is CO_2 concentration after conservative mixing of the ocean and river end members, and $[CO_2]_{mixing\ w/o}$ is CO_2 concentration after the ocean end member is diluted only by a zero DIC freshwater.

In summary, the seasonal changes of pCO_2 in these marine-dominated estuaries are controlled mainly by the annual cycle of water temperature as well as salt marsh production and remineralization processes. In spring and early summer, organic carbon accumulates in the salt marshes because of high *Spartina* productivity (Dai and Wiegert 1996). In late summer and fall, the higher water temperature and greater availability of labile organic matter contribute to higher bacterial remineralization rates in the intertidal marshes (Middelburg et al. 1996; Cai et al. 1999; Wang and Cai 2004). The transport of CO_2 released from intertidal marshes to the estuaries at this time of the year enhances temperature-normalized pCO_2 (Fig. 7). The annual temperature cycle further helps to shape the seasonal variations of in situ pCO_2 in these estuaries.

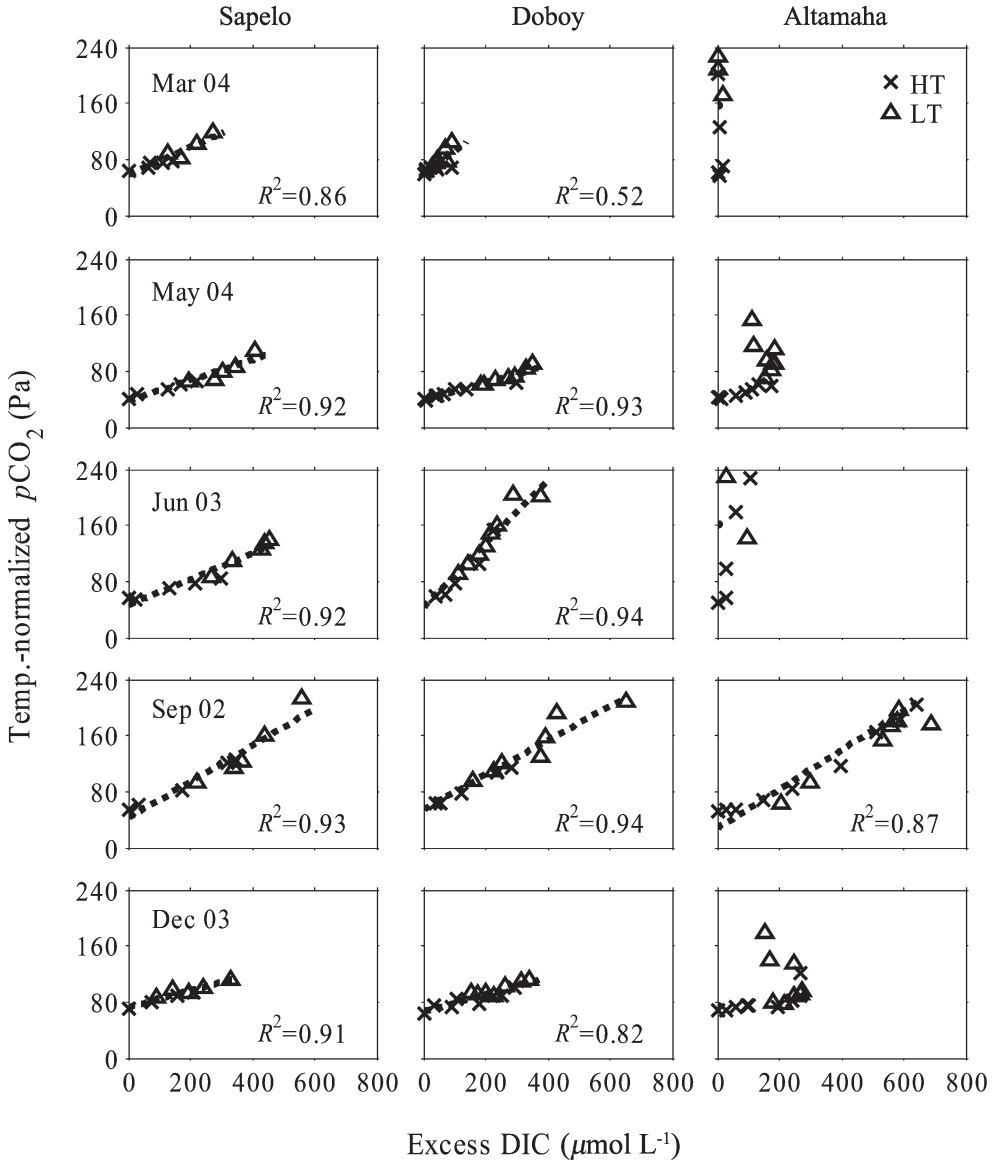

Fig. 9. Temperature-normalized pCO_2 (T = 22.63°C) plotted against excess DIC in Sapelo, Doboy, and Altamaha Sounds. Crosses are data from high-tide (HT) survey, and triangles are data from low-tide (LT) survey.

CO_2 in river-dominated estuaries—pCO_2 in Altamaha Sound was higher than that in the two marine-dominated estuaries during all sampling months (in particular, the high-flow months). Temperature-normalized pCO_2 in Altamaha Sound shows different seasonal trends compared to Sapelo and Doboy Sounds (Fig. 7). Instead of peaking in the warmest months of June 2003 and September 2002, temperature-normalized pCO_2 in Altamaha Sound reached maxima during March 2004 and June 2003, when river discharge rates were highest (Fig. 7). The apparent seasonal covariation of temperature-normalized pCO_2 (Fig. 7) and river discharge rates (Fig. 3b) in Altamaha Sound suggests the importance of freshwater runoff to CO_2 in this type of estuary.

Freshwater runoff from land is an important source of CO_2 to river-dominated estuaries (Raymond et al. 2000; Borges et al. 2006). River water entering estuaries is usually supersaturated with CO_2 (Abril and Borges 2004). Sources of CO_2 in the river include microbial decomposition of organic matter in soils, river waters, and sediments (Cole and Caraco 2001). High concentrations of humic substances also contribute to the high pCO_2 in river water by increasing acidity of source waters (Cai and Wang 1998).

The relative contributions of CO_2 from within the estuarine zone and the river can be calculated. Specifically, CO_2 concentration that is due to inputs from within the estuarine zone ($\Delta[CO_2]_{estuarine}$) can be estimated by the difference between the in situ CO_2 concentration ($[CO_2]_i$) and the CO_2 concentration if only conservative mixing occurs between the ocean and river end members ($[CO_2]_{mixing\ w/R}$) (Fig. 8b). Similarly, CO_2 concentration that is due to input from the river ($\Delta[CO_2]_{river}$) can be

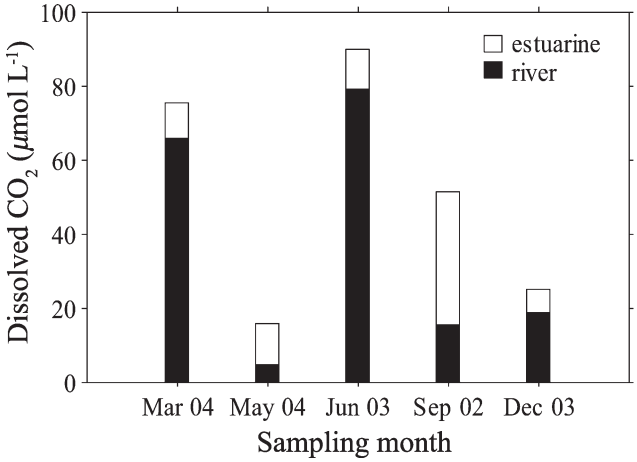

Fig. 10. Dissolved CO_2 concentration (normalized to 22.63°C, area averaged) that is due to inputs from the river and within the estuarine zone (intertidal marsh, net ecosystem metabolism, and all other sources except the ocean and river end members) in Altamaha Sound at low tide. Open columns represent CO_2 from within the estuarine zone; and filled columns represent CO_2 from the river.

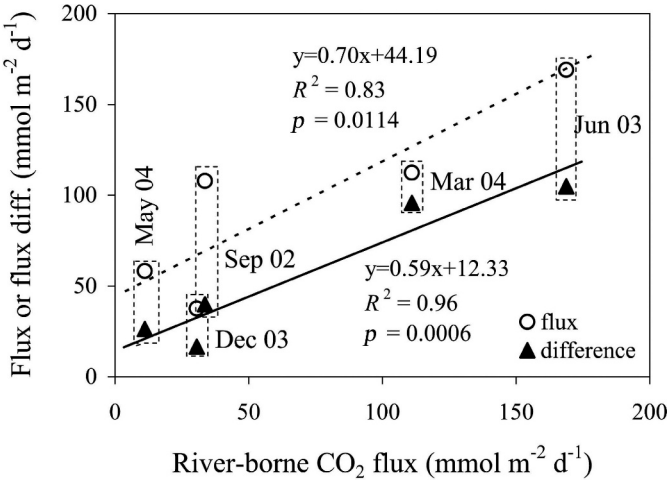

Fig. 11. Air–water CO_2 fluxes in Altamaha Sound and the flux differences between the two types of estuaries against the river-borne CO_2 fluxes. Open circles are air–water CO_2 fluxes in Altamaha Sound at low tide, and filled triangles are the flux differences between the two types of estuaries at low tide. Dotted line is from a model II regression of air–water CO_2 fluxes against the river-borne CO_2 fluxes. Solid line is from a model II regression of the flux differences against the river-borne CO_2 fluxes.

estimated by the difference between $[CO_2]_{mixing\ w/R}$ and the CO_2 concentration if the ocean end member is diluted only by a zero DIC freshwater ($[CO_2]_{mixing\ w/o}$) (Fig. 8b).

As $[CO_2]$ change is not linear during mixing (Fig. 8b), $[CO_2]_{mixing\ w/o}$ and $[CO_2]_{mixing\ w/R}$ cannot be estimated from the CO_2 mixing line directly. However, they can be estimated indirectly based on the fact that DIC and TA mix conservatively with salinity and $[CO_2]$ can be calculated from its corresponding DIC and TA values. Specifically, $[CO_2]_{mixing\ w/o}$ was calculated from $DIC_{mixing\ w/o}$ and $TA_{mixing\ w/o}$, the former of which was estimated according to Eq. 6 (Fig. 8a) and the latter of which was also estimated from Eq. 6 simply by replacing DIC with TA. Similarly, $[CO_2]_{mixing\ w/R}$ was calculated from $DIC_{mixing\ w/R}$ and $TA_{mixing\ w/R}$, both of which were calculated from Eq. 7 (Fig. 8a). When CO_2 concentrations were calculated from DIC and TA, the annual average temperature of 22.63°C was used since the dissolved CO_2 concentration is subject to changes in water temperature.

The results show that CO_2 inputs from within the estuarine zone as well as the river jointly contribute to the CO_2 in river-dominated estuaries (Fig. 10). Their relative importance is most likely a function of water residence time in the estuary (Borges et al. 2006). During high-flow months (March 2004 and June 2003), CO_2 inputs from the river dominate, while inputs from the estuarine zone are less important because of the short water residence time (Fig. 10). On the other hand, during low-flow seasons (May 2004, September 2002, and December 2003), with diminished riverine influence, CO_2 inputs from within the estuarine zone become relatively more important (Fig. 10). Overall, CO_2 inputs from the river are dependent mainly on river discharge rates, while CO_2 inputs from the estuarine zone depend mainly on the season and water residence time (Fig. 10).

The contribution of river-borne CO_2 to overall CO_2 fluxes in river-dominated estuaries was first estimated by Borges et al. (2006) based on the concept of excess CO_2. Excess CO_2 was defined as the quantity of DIC that would transfer to the atmosphere as CO_2 after complete water–air equilibrium (Abril et al. 2000). Potential CO_2 fluxes from the upstream river were then calculated as the product of excess CO_2 and average river discharge rates divided by the estuarine surface area (Borges et al. 2006). However, this method assumed that excess CO_2 varies linearly during mixing, which may not be the case because of the thermodynamic equilibrium of the inorganic carbon system.

For this study, CO_2 fluxes contributed by the river at each sampling station (referred to as river-borne CO_2 fluxes hereafter) were estimated using a new method. Air–water CO_2 flux can be expressed as follows:

$$F = k([CO_{2w}] - [CO_{2a}]) \quad (8)$$

where k is the gas transfer velocity and $[CO_{2w}]$ and $[CO_{2a}]$ are the CO_2 concentration at the bottom and top of the aqueous mass boundary layer, respectively. Assuming that $[CO_{2a}]$ is a constant, we differentiated both sides of Eq. 8 to derive the following:

$$\Delta F = k \cdot \Delta[CO_{2w}] \quad (9)$$

Eq. 9 calculates the change in air–water CO_2 flux when a certain change in surface water CO_2 concentration ($\Delta[CO_{2w}]$) occurs. Since we had already calculated the dissolved CO_2 concentrations that are contributed by the river ($\Delta[CO_2]_{river}$), the corresponding fluxes contributed by the river (ΔF_{river}) can be easily estimated from Eq. 9.

Air–water CO_2 fluxes in Altamaha Sound were plotted against the river-borne CO_2 fluxes (Fig. 11). The positive

correlation shows the importance of river-borne CO_2 to the air–water CO_2 fluxes in river-dominated estuaries. However, their poor linearity ($R^2 = 0.83$) also suggests that CO_2 inputs from other sources (i.e., within the estuarine zone) contribute to the CO_2 fluxes in Altamaha Sound.

To determine whether CO_2 contributed by the river is responsible for the extra-high CO_2 fluxes in the river-dominated estuary, we examined the flux differences in the two types of estuaries and plotted them against the calculated river-borne CO_2 fluxes. The flux differences were estimated as the air–water CO_2 fluxes in Altamaha Sound minus the average fluxes in Sapelo and Doboy Sounds (Table 2). The strong correlation between the flux differences and the river-borne CO_2 fluxes ($R^2 = 0.96$) suggests that CO_2 inputs from the river are likely to be responsible for the extra-higher CO_2 degassing in the river-dominated estuary relative to the two marine-dominated estuaries (Fig. 11).

The data also show that the river-borne CO_2 fluxes are more than enough to account for the flux differences between these two types of estuaries (Fig. 11), indicating that other processes must contribute to the flux differences. Even though the river-dominated estuary gets extra CO_2 from freshwater runoff, it may receive relatively less CO_2 from within the estuarine zone because of its shorter residence time and smaller ratio of salt marsh area to estuarine volume. Plus, estuarine net ecosystem metabolism may also be different between these two types of estuaries because of extra inputs of nutrients and organic matter from the river into the river-dominated estuaries.

Implications to the estimation of global CO_2 fluxes from estuaries—This study shows large differences in CO_2 degassing between river- and marine-dominated estuaries. Higher CO_2 degassing in estuaries that are more influenced by freshwater was also found in other regions of the world, such as the three estuaries in the Cantabrian Sea (north of Spain) (Ortega et al. 2005) and the estuaries in Kaneohe Bay, Oahu, Hawaii (Fagan and Mackenzie 2007). If the conclusion of this study can be applied globally, one implication is that the current estimates of global air–water CO_2 fluxes from estuaries could be overestimated.

The global air–water CO_2 fluxes from estuaries were synthesized by Borges (2005) and Borges et al. (2005) as about +0.40 Pg C yr^{-1}. However, there might be problems associated with these pioneering global estimates. First, the air–water CO_2 fluxes used for the synthesis were mainly from river-dominated estuaries (of small and intermediate-sized rivers) (Borges 2005; Borges et al. 2005). Second, the surface area of global estuaries used included both river- and marine-dominated estuaries (Woodwell et al. 1973). Since air–water CO_2 fluxes in marine-dominated estuaries could be considerably lower than those in river-dominated estuaries, the estimates by Borges (2005) and Borges et al. (2005) might be an overestimation.

Globally, estuaries are far more complicated than being simply classified as either river- or marine-dominated estuaries. Abril and Borges (2004) and Borges (2005) also demonstrated large CO_2 differences between macrotidal and microtidal estuaries. In addition, there are estuaries that are dominated by large rivers, such as those of the Amazon River (Cooley et al. 2007), the Mississippi River (Cai 2003; W.-J. Cai unpubl.), and the Yangtze River (Zhai et al. 2007), where the estuaries are usually weaker CO_2 sources compared to most small and intermediate river-dominated estuaries that have been studied. There are also large estuarine systems, such as Chesapeake Bay, Long Island Sound, Pamlico Sound, and Puget Sound, the surface areas of which cover a large proportion of the total surface area of global estuaries but have generally been understudied. More work is clearly needed to better constrain the global air–water CO_2 fluxes from estuaries.

References

Abril, G., and A. V. Borges. 2004. Carbon dioxide and methane emissions from estuaries, p. 187–207. *In* A. Tremblay, L. Varfalvy, C. Roehm and M. Garneau [eds.], Greenhouse gases emissions from natural environments and hydroelectric reservoirs: Fluxes and processes. Springer.

———, H. Etcheber, A. V. Borges, and M. Frankignoulle. 2000. Excess atmospheric carbon dioxide transported by rivers into the Scheldt estuary. Earth Planet. Sci. **330:** 761–768.

Borges, A. V. 2005. Do we have enough pieces of the jigsaw to integrate CO_2 fluxes in the coastal ocean? Estuaries **28:** 3–27.

———, B. Delille, and M. Frankignoulle. 2005. Budgeting sinks and sources of CO_2 in the coastal ocean: Diversity of ecosystems counts. Geophys. Res. Lett. **32:** L14601, doi:10.1029/2005GL023053.

———, B. Delille, L. S. Schiettecatte, F. Gazeau, G. Abril, and M. Frankignoulle. 2004*a*. Gas transfer velocities of CO_2 in three European estuaries (Randers Fjord, Scheldt and Thames). Limnol. Oceanogr. **49:** 1630–1641.

———, L.-S. Schiettecatte, G. Abril, B. Delille, and F. Gazeau. 2006. Carbon dioxide in European coastal waters. Estuar. Coast. Shelf Sci. **70:** 375–387.

———, J.-P. Vanderborght, L.-S. Schiettecatte, F. Gazeau, S. Ferrón-Smith, B. Delille, and M. Frankignoulle. 2004*b*. Variability of the gas transfer velocity of CO_2 in a macrotidal estuary (the Scheldt). Estuaries **27:** 593–603.

Cai, W.-J. 2003. Riverine inorganic carbon flux and rate of biological uptake in the Mississippi River plume. Geophys. Res. Lett. **30:** 1032, doi:10.1029/2002GL016312.

———, M. Dai, and Y. Wang. 2006. Air-sea exchange of carbon dioxide in ocean margins: A province-based synthesis. Geophys. Res. Lett. **33:** L12603, doi:10.1029/2006GL026219.

———, L. R. Pomeroy, M. A. Moran, and Y. Wang. 1999. Oxygen and carbon dioxide mass balance for the estuarine-intertidal marsh complex of five rivers in the southeastern U.S. Limnol. Oceanogr. **44:** 639–649.

———, and Y. Wang. 1998. The chemistry, fluxes, and sources of carbon dioxide in the estuarine waters of the Satilla and Altamaha Rivers, Georgia. Limnol. Oceanogr. **43:** 657–668.

———, Z. A. Wang, and Y. Wang. 2003. The role of marsh-dominated heterotrophic continental margins in transport of CO_2 between the atmosphere, the land-sea interface and the ocean. Geophys. Res. Lett. **30:** 1849, doi:10.1029/2003GL017633.

Cameron, W. M., and D. W. Pritchard. 1963. Estuaries, p. 306–324. *In* M. N. Hill [ed.], The sea. V 2. John Wiley & Sons.

Carini, S., N. Wetson, C. S. Hopkins, J. Tucker, A. Giblin, and J. Vallino. 1996. Gas exchange in the Parker Estuary, Massachusetts. Biol. Bull. **191:** 333–334.

Clark, J. F., R. Wanninkhof, P. Schlosser, and H. J. Simpson. 1994. Gas exchange rates in the tidal Hudson river using a dual tracer technique. Tellus **46:** 274–285.

Cole, J. J., and N. F. Caraco. 2001. Carbon in catchments: Connecting terrestrial carbon losses with aquatic metabolism. Mar. Freshw. Res. **52:** 101–110.

Cooley, S. R., V. J. Coles, A. Subramaniam, and P. L. Yager. 2007. Seasonal variations in the Amazon plume-related atmospheric carbon sink. Glob. Biogeochem. Cycles **21:** GB3014, doi:10.1029/2006GB002831.

Dai, T., and R. G. Wiegert. 1996. Estimation of the primary productivity of Spartina alterniflora using a canopy model. Ecography **19:** 410–423.

Elliott, M., and D. S. McLusky. 2002. The need for definitions in understanding estuaries. Estuar. Coast. Shelf Sci. **55:** 815–827.

Elsinger, R. J., and W. S. Moore. 1983. Gas exchange in the Pee Dee River based on ^{222}Rn evasion. Geophys. Res. Lett. **10:** 443–446.

Fagan, K. E., and F. T. Mackenzie. 2007. Air-sea CO_2 exchange in a subtropical estuarine-coral reef system, Kaneohe Bay, Oahu, Hawaii. Mar. Chem. **106:** 174–191.

Frankignoulle, M., G. Abril, A. Borges, I. Bourge, C. Canon, B. Delille, E. Libert, and J.-M. Théate. 1998. Carbon dioxide emission from European estuaries. Science **282:** 434–436.

Guérin, F., and others. 2007. Gas transfer velocities of CO_2 and CH_4 in a tropical reservoir and its river downstream. J. Mar. Syst. **66:** 161–172.

Hartman, B., and D. H. Hammond. 1984. Gas exchange across the sediment-water and air-water interfaces in south San Francisco Bay. J. Geophys. Res. **89:** 3593–3603.

Ho, D. T., C. S. Law, M. J. Smith, P. Schlosser, M. Harvey, and P. Hill. 2006. Measurements of air-sea gas exchange at high wind speeds in the Southern Ocean: Implications for global parameterizations. Geophys. Res. Lett. **33:** L16611, doi:10.1029/2006GL026817.

Jahnke, R. A., C. R. Alexander, and J. E. Kostka. 2003. Advective pore water input of nutrients to the Satilla River Estuary, Georgia, USA. Estuar. Coast. Shelf Sci. **56:** 641–653.

Jiang, L.-Q., W.-J. Cai, R. Wanninkhof, Y. Wang, and H. Lüger. 2008. Air-sea CO_2 fluxes on the U.S. South Atlantic Bight: spatial and seasonal variability. J. Geophys. Res **113:** C07019, doi:10.1029/2007JC004366.

Kremer, J. N., A. Peischauer, and C. D'avanzo. 2003. Estuary-specific variation in the air-water gas exchange coefficient for oxygen. Estuaries **26:** 829–836.

Marino, R., and R. W. Howarth. 1993. Atmospheric oxygen exchange in the Hudson river: Dome measurements and comparison with other natural waters. Estuaries **16:** 433–445.

Middelburg, J. J., G. Klaver, J. Nieuwenhuize, A. Wielemaker, W. De Hass, T. Vlug, and F. W. AVan Der Nat. 1996. Organic matter mineralization in intertidal sediments along an estuarine gradient. Mar. Ecol. Prog. Ser. **132:** 157–168.

National Ocean Service. 1985. National estuarine inventory data atlas, V 1: Physical and hydrologic characteristics. National Ocean Service, NOAA, U.S. Department of Commerce.

Neubauer, S., and I. C. Anderson. 2003. Transport of dissolved inorganic carbon from a tidal freshwater marsh to the York River estuary. Limnol. Oceanogr. **48:** 299–307.

Ortega, T., R. P. J. Forja, and Gómez-Parra. 2005. Fluxes of dissolved inorganic carbon in three estuarine systems of the Cantabrian Sea (north of Spain). J. Mar. Syst. **53:** 125–142.

Perillo, G. M. E. 1995. Definitions and geomorphologic classifications of estuaries, p. 17–47. *In* G. M. E. Perillo [ed.], Geomorphology and sedimentology of estuaries. Elsevier.

Raymond, P. A., J. E. Bauer, and J. J. Cole. 2000. Atmospheric CO_2 evasion, dissolved inorganic carbon production, and net heterotrophy in the York River estuary. Limnol. Oceanogr. **45:** 1707–1717.

———, and J. J. Cole. 2001. Gas exchange in rivers and estuaries: Choosing a gas transfer velocity. Estuaries **24:** 312–317.

Roques, P. F. 1985. Rate and stoichiometry of nutrient remineralization in an anoxic estuary, the Pettaquamscutt River.Ph.D. thesis. Univ. of Rhode Island.

Takahashi, T., J. Olafsson, J. G. Goddard, D. W. Chipman, and S. C. Sutherland. 1993. Seasonal variation of CO_2 and nutrients in the high-latitude surface oceans: A comparative study. Glob. Biogeochem. Cycles **7:** 843–878.

———, and others. In press. Climatological mean and decadal changes in surface ocean pCO_2 and net sea-air CO_2 flux over the global oceans. Deep-Sea Res. II.

Tokoro, T., and others. 2007. Measurement of air-water CO_2 transfer at four coastal sites using a chamber method. J. Mar. Syst. **66:** 140–149.

Tsunogai, S., S. Watanabe, and T. Sato. 1999. Is there a "continental shelf pump" for the absorption of atmospheric CO_2? Tellus **51:** 701–712.

Wang, Z., and W.-J. Cai. 2004. Carbon dioxide degassing and inorganic carbon export from a marsh dominated estuary (the Duplin River): A marsh CO_2 pump. Limnol. Oceanogr. **49:** 341–352.

Wanninkhof, R. 1992. Relationship between gas exchange and wind speed over the ocean. J. Geophys. Res. **97:** 7373–7381.

Woodwell, G. M., P. H. Rich, and C. A. S. Hall. 1973. Carbon in estuaries, p. 221–240. *In* G. M. Woodwell and E. V. Pecan [eds.], Carbon and the biosphere: Proceedings of the 24th Brookhaven Symposium in Biology, Upton. Technical Information Center, U.S. Atomic Energy Commission.

Zappa, C. J., and others. 2007. Environmental turbulent mixing controls on air-water gas exchange in marine and aquatic systems. Geophys. Res. Lett. **34:** L10601, doi:10.1029/2006GL028790.

Zhai, W., M. Dai, and X. Guo. 2007. Carbon system and CO_2 degassing fluxes in the inner estuary of Changjiang (Yangtze) River, China. Mar. Chem. **107:** 342–356.

Received: 17 January 2008
Accepted: 30 April 2008
Amended: 1 July 2008